

A Light-Scattering Study of the Aggregation Behavior of Fluorocarbon-Modified Polyacrylamides in Water

Yubao Zhang,[†] Chi Wu,^{*,†} Qing Fang,[‡] and Yun-Xiang Zhang[‡]

Department of Chemistry, The Chinese University of Hong Kong, Shatin, Hong Kong, and Shanghai Institute of Organic Chemistry, Academia Sinica, Shanghai 200032, China

Received October 24, 1995; Revised Manuscript Received December 12, 1995[®]

ABSTRACT: Fluorocarbon-modified polyacrylamide chains can form large multichain aggregates. The aggregation behavior of a series of fluorocarbon-modified polyacrylamides in water has been investigated by a combination of static and dynamic laser light scattering (LLS). The critical aggregation concentration (CAC) was estimated from the emergence of a second peak in the line-width distribution measured in dynamic LLS. Our results showed that CAC strongly depends on the amount of 2-(*N*-ethylperfluorooctanesulfonamido)ethyl acrylate (FX-13) copolymerized with polyacrylamide and also on the polymer concentration. When the FX-13 content is 0.227 mol %, CAC is as low as 1.34×10^{-4} g/mL, while when the FX-13 content is less than 0.028 mol %, no aggregation has been observed over the entire concentration range studied. A combination of the weight-average molecular weight from static LLS and the area ratio of the two peaks in the line-width distribution from dynamic LLS leads us to the estimation that on average each aggregate consists of ~ 5 –9 individual polymer chains for the acrylamide copolymer with 0.227 mol % FX-13. The solution contained 40 wt % of the multichain aggregates when the polymer concentration was higher than the CAC. On the other hand, the intensity ratio of the light scattered from the multichain aggregates over that from individual chains increased linearly with increasing polymer concentration.

Introduction

Hydrophobically modified water soluble polymers exhibit unusual rheological features that are markedly different from those of the unmodified parent polymers. Besides their numerous applications, such as in water treatment, as flocculating agents, and in enhanced oil recovery, the fundamental question relating to the aggregation of these polymers and the fact that these synthetic polymers can be used as models for the understanding of the behavior of more complicated biological macromolecules has attracted much attention.^{1–8} Many previous researches have focused on the copolymers made of acrylamide and comonomers containing long hydrocarbon chains, such as *N*-alkylacrylamide. It has been found that the incorporation of only ~ 1 mol % of octylacrylamide into acrylamide could lead to a substantial increase in the solution viscosity.⁸ Zhang and co-workers reported the preparation of a series of copolymers made of acrylamide and fluorocarbon-containing acrylates.⁹ Replacing hydrogen with fluorine resulted in an enhancement of the hydrophobic character of the copolymers, resulting in a much larger viscosity enhancement in comparison with the corresponding polyacrylamide modified with the hydrocarbon chain. This viscosity enhancement has been generally attributed to the association of the hydrophobic side groups in aqueous solution. However, a better understanding of this hydrophobic association is much needed. In the past, besides the viscosity measurement, other modern experimental methods including dynamic laser light scattering¹⁰ were used to study the aggregation of the modified polyacrylamides in water. It is generally known that the aggregation can be influenced by both the fluorocarbon monomer content and polymer concentration. To our knowledge, the transition from individual copolymer chains to multichain aggregates has

not been observed yet, and the aggregation mechanism has not been studied in detail.

In this study, the aggregation of a series fluorocarbon modified polyacrylamides in water over a wide range of polymer concentrations was investigated by a combination of static and dynamic laser light scattering (LLS). We focused on two problems: (1) the transition from individual polymer chains to multichain aggregates; and (2) how the structure and weight fraction of the multichain aggregates are influenced by the fluorocarbon content and polymer concentration.

Experimental Section

Sample Preparation. Ultrapure electrophoresis grade acrylamide purchased from Polysciences Inc. was used without further purification. The fluorine-containing surfactant potassium perfluorooctanecarboxylate (FC-143) and monomer 2-(*N*-ethylperfluorooctanesulfonamido)ethyl acrylate [$\text{CH}_2=\text{CH}_2\text{C}(\text{O})\text{OCH}_2\text{CH}_2\text{N}(\text{C}_2\text{H}_5)\text{SO}_2\text{C}_8\text{F}_{17}$, denoted as FX-13] (courtesy of 3M) were recrystallized from methanol. All solvents and salts used were of reagent grade.

The copolymerization of acrylamide and FX-13 were detailed before.⁹ Into a 100-mL flask were added 8 mL of acetone containing a proper amount of FX-13, 4 g of acrylamide, 100 mg of FC-143, and 40 mL of deionized water. The mixture was stirred and heated to 50 °C. After purging the mixture with N_2 for 30 min, 1 mL of $(\text{NH}_4)_2\text{SO}_4$ (0.465 g/mL of aqueous solution) was injected and the reaction was carried out for 24 h. At the end of the polymerization, the solution was diluted with deionized water. The copolymer was precipitated in acetone and dried in vacuum at 40 °C for 24 h. The copolymers were further purified twice by dissolution in deionized water, filtration with 5- μm Millipore filter, and precipitation into acetone. The molar ratio of FX-13/acrylamide in the copolymer ranged from 0.028% to 0.227%.

All solutions used in laser light scattering were prepared by dissolving a proper amount of the copolymer in deionized water whose electric conductivity was 18.3 M Ω cm. The solutions were clarified by a 0.8- μm Millipore filter, except for a few concentrated solutions ($C \geq 5 \times 10^{-3}$ g/mL), where the ultracentrifuge (2×10^4 g) was used.

Laser Light Scattering (LLS). A modified commercial LLS spectrometer (ALV/SP-125) equipped with a multi-tau digital time correlator (ALV-5000) and a solid-state laser

* To whom correspondence should be addressed.

[†] The Chinese University of Hong Kong.

[‡] Academia Sinica.

[®] Abstract published in *Advance ACS Abstracts*, February 15, 1996.

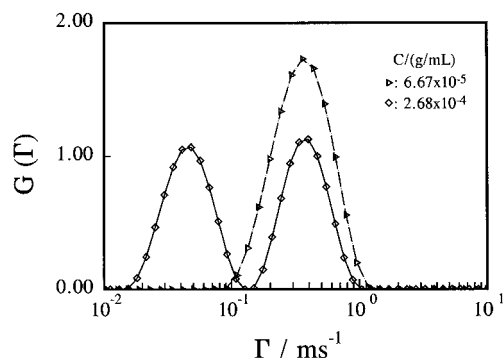


Figure 1. Concentration dependence of the line-width distribution $G(\Gamma)$ for the copolymer containing 0.227 mol % of 2-(*N*-ethylperfluorooctanesulfonamido)ethyl acrylate (FX-13).

(ADLAS DPY 425 II, output power ≈ 400 mW at $\lambda_0 = 532$ nm) were used in this study. The incident beam was vertically polarized with respect to the scattering plane. All measurements were carried out at 25.0 ± 0.1 °C. The refractive index increment (dn/dc) was determined by a novel and precise differential refractometer.¹¹

In static LLS, the angular dependence of the excess absolute time-averaged scattered intensity, known as the excess Rayleigh ratio $R_{vv}(q)$, of a set of dilute copolymer solutions was measured. $R_{vv}(q)$ is related to the weight-average molecular weight M_w , the second virial coefficient A_2 , and the z -average radius of gyration $\langle R_g^2 \rangle_z^{1/2}$ (or written as $\langle R_g \rangle$) by¹²

$$\frac{KC}{R_{vv}(q)} \approx \frac{1}{M_w} \left(1 + \frac{1}{3} \langle R_g^2 \rangle q^2 \right) + 2A_2 C \quad (1)$$

where $K = 4\pi^2 n^2 (dn/dc)^2 / (N_A \lambda_0^4)$, with N_A , n , and λ_0 being Avogadro's constant, the solvent refractive index, and the wavelength of light in vacuum, respectively. $q = (4\pi n / \lambda_0) \sin(\theta/2)$, θ being the scattering angle. The copolymer concentration is given in g/mL.

In dynamic LLS, the intensity–intensity time correlation function $G^{(2)}(t, q)$ in the self-beating mode was measured. $G^{(2)}(t, q)$ can be related to the normalized first-order electric field time correlation function $|g^{(1)}(t, q)|$ by^{13,14}

$$G^{(2)}(t, q) = \langle I(0, q) I(t, q) \rangle = A [1 + \beta |g^{(1)}(t, q)|^2] \quad (2)$$

where A is a measured baseline; β , a parameter depending on the coherence of the detection; and t , the delay time. For a polydisperse sample, $|g^{(1)}(t, q)|$ is further related to the line-width distribution $G(\Gamma)$ by

$$|g^{(1)}(t, q)| = \langle E(0, q) E^*(t, q) \rangle = \int_0^\infty G(\Gamma) e^{-\Gamma t} d\Gamma \quad (3)$$

$G(\Gamma)$ can be calculated from $G^{(2)}(t, q)$ on the basis of eqs 2 and 3 by using the constrained regularization CONTIN program developed by Provencher.¹⁵ For a diffusive relaxation, Γ is a function of both C and q , i.e.,^{16,17}

$$\Gamma/q^2 = D(1 + k_d C)(1 + f \langle R_g^2 \rangle q^2) \quad (4)$$

where D is the translational diffusion coefficient at $C \rightarrow 0$ and $q \rightarrow 0$; f , a dimensionless constant; and k_d , the diffusion second virial coefficient. D , f , and k_d can be obtained from $(\Gamma/q^2)_{C \rightarrow 0, q \rightarrow 0}$, $(\Gamma/q^2)_{C \rightarrow 0}$ vs q^2 , and $(\Gamma/q^2)_{q \rightarrow 0}$ vs C , respectively. Further, D is related to the hydrodynamic radius (R_h) by the Stokes–Einstein equation: $R_h = k_B T / 6\pi\eta D$, where η is the solvent viscosity; k_B , the Boltzmann constant; and T , the absolute temperature.

Results and Discussion

The Critical Aggregation Concentration (CAC).

Figure 1 shows a typical concentration dependence of

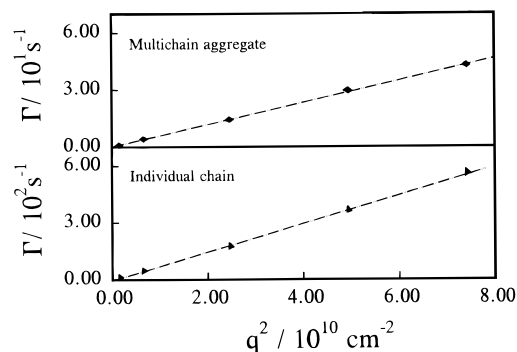


Figure 2. Angular dependence of the average line width $\langle \Gamma \rangle$ for the two peaks shown in Figure 1.

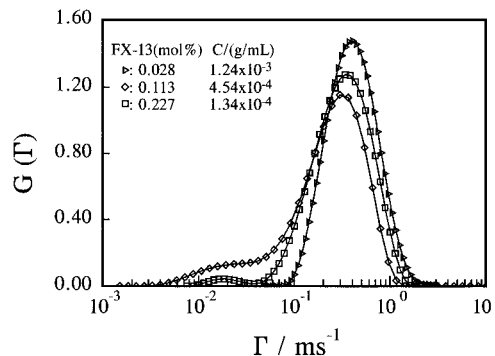


Figure 3. Line-width distributions near the critical aggregation concentration (CAC) for copolymers with different 2-(*N*-ethylperfluorooctanesulfonamido)ethyl acrylate (FX-13) contents.

the line-width distributions $G(\Gamma)$ for the copolymer containing 0.227 mol % of FX-13. When $C \leq 1.00 \times 10^{-4}$ g/mL, only one peak was detected in $G(\Gamma)$. As C increases, a second peak with a small average Γ appears. The second peak represents a much slower relaxation process in comparison with the relaxation related to the first peak.

Figure 2 shows typical plots of the average line width $\langle \Gamma \rangle$ versus q^2 , respectively, for each of the two peaks in Figure 1. The linear dependence of $\langle \Gamma \rangle$ on q^2 indicates that the relaxations related to both the peaks are diffusive. The peak with a larger $\langle \Gamma \rangle$ is related to the translational diffusion of individual copolymer chains, while the peak with a smaller $\langle \Gamma \rangle$ can be attributed to the translational diffusion of larger multichain aggregates. The calculated apparent average hydrodynamic radius (R_h) for individual copolymer chains is ~ 40 nm, while for the multichain aggregates it is in the range of ~ 300 – 500 nm. For a given FX-13 content, the area ratio of the two peaks in Figure 1 is a function of copolymer concentration.

Figure 3 shows typical line-width distributions for three copolymers with different FX-13 contents, wherein the second peak is just emerged into $G(\Gamma)$. The concentration corresponding to the second peak is defined as the critical aggregation concentration (CAC). When the FX-13 content is less than 0.028 mol %, no aggregation was detectable over the entire concentration range studied. The estimated values of CAC for the copolymers with different FX-13 contents are listed in Table 1.

The Multichain Aggregates. Panels (a) and (b) of Figure 4 show typical Zimm plots for polyacrylamide containing 0 mol % (i.e., homopolymer) and 0.227 mol % of FX-13, respectively. On the basis of eq 1, we were

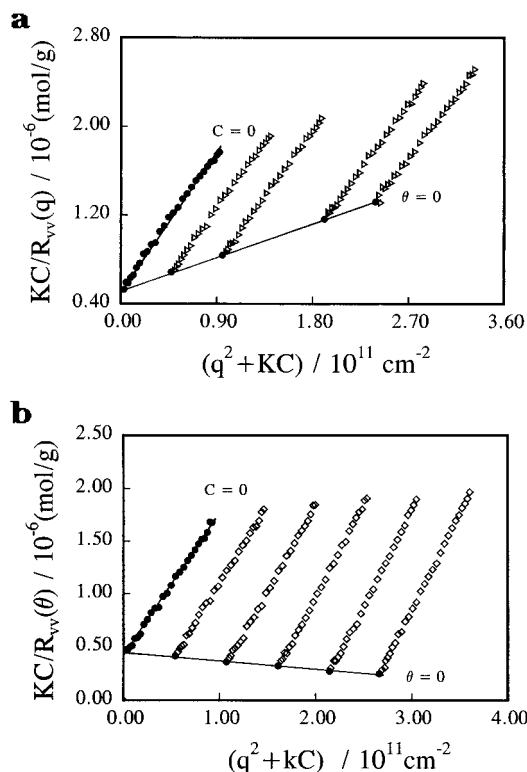


Figure 4. Typical Zimm plot for polyacrylamide containing (a) 0 mol % of FX-13 (homopolymer), where the copolymer concentration ranges from 2.39×10^{-4} to 1.19×10^{-3} g/mL; (b) 0.227 mol % of FX-13 (copolymer), where the copolymer concentration ranges from 2.68×10^{-4} to 1.34×10^{-3} g/mL.

Table 1. Light Scattering Results of PAM-co-(FX-13) in Water at 25 °C

sample	FX-13 (mol %)	M_w (10^6 g/mol)	A_2 (10^{-4} ml·mol $^{-1}$ ·g $^{-2}$)	R_g (nm)	CAC (10^{-4} g/mL)
PA1	0	1.91	3.4	89	
PA2	0.028	1.66	3.9	79	
PA3	0.113	2.22	-2.0	104	~4.5
PA4	0.227	2.16	-1.1	95	~1.3

able to calculate M_w , R_g , and A_2 from the extrapolation of $[KC/R_{vv}(q)]_{q \rightarrow 0, C \rightarrow 0}$, $[KC/R_{vv}(q)]_{C \rightarrow 0}$ vs q^2 and $[KC/R_{vv}(q)]_{q \rightarrow 0}$ vs C , respectively. The results are summarized in Table 1. A comparison of panels (a) and (b) of Figure 4 shows that as the FX-13 content increases, A_2 changed from positive to negative, indicating that water changed from a good solvent to a poor solvent. This is why the aggregation was detected in dynamic LLS. It should be noted that $\langle R_g \rangle$ and A_2 listed in Table 1 indicate the contributions from both individual single chains and multichain aggregates.

It has been shown that a combination of static and dynamic LLS results can provide information on the aggregation number as well as the weight fraction of the aggregates in the solution.^{18,19,20} The following is the outline of its basic principle. On the basis of eqs 1 and 3, at $t \rightarrow 0$, $q \rightarrow 0$, and a finite C , we have

$$|g^{(1)}(0, q)| = \int_0^\infty G(\Gamma) d\Gamma \propto \langle I \rangle \propto R_{vv}(q \rightarrow 0) \propto M_w^* C \quad (5)$$

where $M_w^* [=M_w(1 - 2A_2M_wC)]$ is an apparent weight-average molecular mass at a finite C . Equation 5 shows that the peak area in $G(\Gamma)$ is proportional to the excess scattered intensity. For a polymer mixture of individual chains and multichain aggregates, we denote the two

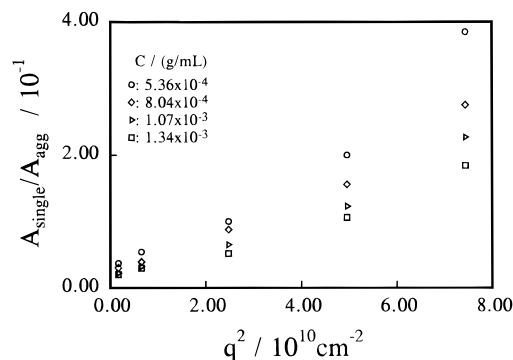


Figure 5. Angular dependence of the area ratio of the two peaks shown in Figure 1.

peaks in $G(\Gamma)$ as $G_{\text{single}}(\Gamma)$ and $G_{\text{agg}}(\Gamma)$; then, the area ratio A_r of these two peaks is

$$A_r = \frac{A_{\text{single}}}{A_{\text{agg}}} = \frac{\int_\gamma^\infty G_{\text{single}}(\Gamma) d\Gamma}{\int_0^\gamma G_{\text{agg}}(\Gamma) d\Gamma} = \frac{M_{w,\text{single}}^* C_{\text{single}}}{M_{w,\text{agg}}^* C_{\text{agg}}} = \frac{M_{w,\text{single}}^* x_{\text{single}}}{M_{w,\text{agg}}^* x_{\text{agg}}} \quad (6)$$

where γ is the cutoff line width between $G_{\text{single}}(\Gamma)$ and $G_{\text{agg}}(\Gamma)$; x_{single} and x_{agg} are the weight fractions of individual chains and multichain aggregates, respectively; and $x_{\text{single}} + x_{\text{agg}} = 1$. On the other hand, in the static LLS, the extrapolation of $[KC/R_{vv}(q)]_{q \rightarrow 0}$ for each finite concentration C leads to an M_w^* at that concentration which contains contributions from both individual chains and multichain aggregates, i.e.,

$$M_w^* = M_{w,\text{single}}^* x_{\text{single}} + M_{w,\text{agg}}^* x_{\text{agg}} \quad (7)$$

On the basis of eqs 6 and 7, a combination of M_w^* from static LLS and $A_r, q \rightarrow 0$ from dynamic LLS can lead to $M_{w,\text{single}}^* x_{\text{single}}$ and $M_{w,\text{agg}}^* x_{\text{agg}}$. In principle, after knowing any one of the four parameters ($M_{w,\text{single}}^*$, $M_{w,\text{agg}}^*$, x_{single} , and x_{agg}), we will be able to determine the rest of the three parameters from M_w^* and $A_r, q \rightarrow 0$. In this study, we know $M_{w,\text{single}}^*$ from $M_{w,\text{single}}$ and A_2 obtained at infinite dilution.

Figure 5 shows the angular dependence of the area ratio $A_{\text{single}}/A_{\text{agg}}$ for the copolymer with 0.227 mol % of FX-13 at different copolymer concentrations. It shows that when the scattering angle is small, $A_{\text{single}}/A_{\text{agg}}$ is linearly dependent on q^2 . The extrapolation of A_r to the zero scattering angle in the small angle range leads to $A_r, q \rightarrow 0$. The curvature of $A_{\text{single}}/A_{\text{agg}}$ is expected because, at higher scattering angles, the higher order term related to q^4 starts to contribute to $A_{\text{single}}/A_{\text{agg}}$ as the multichain aggregates are fairly larger.¹⁸ Therefore, the accessible small angle range is crucially important in this kind of study. Figure 6 shows the concentration dependence of $(A_{\text{agg}}/A_{\text{single}})_{q \rightarrow 0}$. As expected, when $C \rightarrow 0$, $[(A_{\text{agg}}/A_{\text{single}})_{q \rightarrow 0}] \rightarrow 0$. It is interesting to note that $(A_{\text{agg}}/A_{\text{single}})_{q \rightarrow 0}$ increases linearly with increasing C . The exact reason behind this linear concentration dependence is unclear.

A combination of M_w^* from Figure 4(b) and $A_r, q \rightarrow 0$ from Figure 5 leads to $M_{w,\text{agg}}^*$ and x_{agg} for each concentration. The calculated values of $M_{w,\text{agg}}^*$ and x_{agg} are summarized in Table 2, where we have used $M_{w,\text{single}} = 1.11 \times 10^6$ g/mol measured at a concentration of 1.61×10^{-5} g/mL, well below the CAC. The weight fraction of the multichain aggregates approaches a constant value

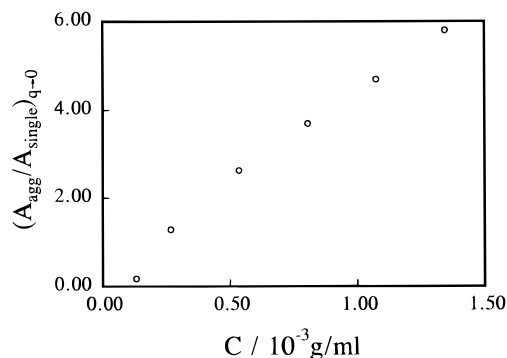


Figure 6. Concentration dependence of the area ratio of the two peaks shown in Figure 1 for the copolymer containing 0.227 mol % of FX-13.

Table 2. Concentration Dependence of Aggregates for PAM-co-(FX-13) (FX-13: 0.227 mol %)

concn (10 ⁻⁴ g/mL)	$M_{w,app}^*$ (10 ⁶ g/mol)	x_{agg}	$M_{w,agg}^*$ (10 ⁶ g/mol)	aggregation no.
2.68	2.2	0.2	5.8	5.3
5.36	2.8	0.4	5.9	5.3
8.04	3.3	0.4	6.7	6.0
10.7	3.8	0.4	7.8	7.1
13.4	4.6	0.4	9.7	8.7

of 0.4 when $C \geq 5.36 \times 10^{-4}$ g/mL. Further increase of the copolymer concentration resulted in larger aggregates. Similar features have also been observed in the aggregation of sulfonated polystyrene ionomers.¹⁹ For a sulfonated polystyrene block copolymer, Zhou *et al.*²⁰ also found the weight fraction of the aggregates is essentially constant over a wide range of polymer concentrations studied. We found that these large aggregates can be removed by filtration. The level-off of the weight fraction of the aggregates at higher copolymer concentration ($\geq 5.36 \times 10^{-4}$ g/mL) might arise from the composition polydispersity of the sample.

In summary, a combination of static and dynamic laser light scattering of the aggregation of a series of fluorocarbon-modified polyacrylamides in aqueous solution has shown that both the fluorocarbon content and polymer concentration have a great influence on the formation (size and weight fraction) of the multichain aggregates. The critical aggregation concentrations (CAC) at which individual copolymer chains start to form the multichain aggregates were determined for the copolymers containing different fluorocarbon contents. The value of CAC ranges from 1.34×10^{-4} to 4.53×10^{-4} g/mL, depending on the fluorocarbon content.

When the fluorocarbon content is lower than 0.028 mol %, no aggregation was detectable over the concentration range studied. Our results show that on average each multichain aggregate contains ~ 5 – 9 chains and the weight fraction of the multichain aggregates ranges from 0% to 40%, depending on the copolymer concentration. The level-off of the weight fraction of the aggregates at higher copolymer concentration might arise from the composition polydispersity of the sample.

Acknowledgment. The financial support of this work by the RGC (the Research Grants Council of the Hong Kong Government) Earmarked Grant 1994/95 (CUHK 299/94P, 221600260) is gratefully acknowledged.

References and Notes

- (1) Glass, J. E. *Polymers in Aqueous Media*; Advances in Chemistry Series No. 223; American Chemical Society: Washington, DC, 1989.
- (2) Shalaby, S. W.; McCormick, C. L.; Butler, G. B. *Water Soluble Polymers*; ACS Symposium Series No. 467; American Chemical Society: Washington, DC, 1991.
- (3) Dubin, P.; Bock, J.; Davis, R.; Schulz, D. N.; Thies, C. *Macromolecular Complex in Chemistry and Biology*; Springer-Verlag: Berlin and Heidelberg, 1994.
- (4) Glass, J. E. *Polym. Mater. Sci. Eng.* **1987**, *57*, 618.
- (5) Evani, S.; Rose, G. D. *Polym. Mater. Sci. Eng.* **1987**, *57*, 477.
- (6) McCormick, C. L.; Hoyle, C. E.; Clark, M. D. *Polym. Mater. Sci. Eng.* **1987**, *57*, 643.
- (7) Landoll, L. M. *J. Polym. Sci., Polym. Chem. Ed.* **1982**, *20*, 443.
- (8) Bock, J.; Siano, D. B.; Schulz, D.; Turner, S. R.; Valint, P. L., Jr.; Pace, S. *Polym. Mater. Sci. Eng.* **1986**, *55*, 355.
- (9) Zhang, Y. X.; Da, A. H.; Butler, G. B.; Hogen-Esch, T. E. *J. Polym. Sci., Polym. Chem. Ed.* **1992**, *30*, 1383.
- (10) Seery, T. A. P.; Yassini, M.; Hogen-Esch, T. E.; Amis, E. J. *Macromolecules* **1992**, *25*, 4784.
- (11) Wu, C.; Xia, K.-Q. *Rev. Sci. Instrum.* **1994**, *65*, 587.
- (12) Zimm, B. H. *J. Chem. Phys.* **1948**, *16*, 1099.
- (13) Berne, B. J.; Pecora, R. *Dynamic Light Scattering*; Wiley: New York, 1976.
- (14) Chu, B. *Laser Light Scattering*; Academic Press: New York, 1974.
- (15) Provencher, S. W. *Makromol. Chem.* **1979**, *180*, 201.
- (16) Stockmayer, W. H.; Schmidt, M. *Pure Appl. Chem.* **1982**, *54*, 407.
- (17) Stockmayer, W. H.; Schmidt, M. *Macromolecules* **1984**, *17*, 509.
- (18) Wu, C.; Mohammad, S.; Woo, K. F. *Macromolecules* **1995**, *28*, 4914.
- (19) Kirill, N. B.; Iwao, T.; William, J. M.; Frank, E. K. *Macromolecules* **1993**, *26*, 1972.
- (20) Zhou, Z.; Peiffer, D. G.; Chu, B. *Macromolecules* **1994**, *27*, 1428.

MA9515792